

Transformer-based Network for RGB-D Saliency Detection

Yue Wang¹, Xu Jia¹, Lu Zhang¹, Yuke Li², James Elder³, Huchuan Lu¹

¹Dalian University of Technology

²UC Berkeley

³York University

Abstract

RGB-D saliency detection integrates information from both RGB images and depth maps to improve prediction of salient regions under challenging conditions. The key to RGB-D saliency detection is to fully mine and fuse information at multiple scales across the two modalities. Previous approaches tend to apply the multi-scale and multi-modal fusion separately via local operations, which fails to capture long-range dependencies. Here we propose a transformer-based network to address this issue. Our proposed architecture is composed of two modules: a transformer-based within-modality feature enhancement module (TWFEM) and a transformer-based feature fusion module (TFFM). TFFM conducts a sufficient feature fusion by integrating features from multiple scales and two modalities over all positions simultaneously. TWFEM enhances feature on each scale by selecting and integrating complementary information from other scales within the same modality before TFFM. We show that transformer is a uniform operation which presents great efficacy in both feature fusion and feature enhancement, and simplifies the model design. Extensive experimental results on six benchmark datasets demonstrate that our proposed network performs favorably against state-of-the-art RGB-D saliency detection methods.

Introduction

RGB-D saliency detection aims at discovering and segmenting the most salient objects accurately in complex scenes by exploiting both RGB image and depth data. It can serve as an early vision step for visual tracking (Lee and Kim 2018), object detection (Xu et al. 2015), content-aware image editing (Wang, Shen, and Ling 2018), and image retrieval (He et al. 2012).

RGB images capture both color cues and texture details of objects that may be sufficient to distinguish foreground objects from background in some simple scenes. However, it may not work for highly cluttered scenes or scenes in which foreground and background share similar colors and textures. Depth maps, on the other hand, would benefit the discovering and segmenting process for these complex scenes. It records the distance of different objects in a scene to the camera, which provides an additional cue to capture the spatial structure and 3D layout. Therefore, information provided by RGB images and depth maps are complementary

to each other. Effective fusion of information from such two modalities can be critical for accurate saliency detection.

Inspired by the success of deep learning methods, RGB-D saliency detection apply CNN models (Simonyan and Zisserman 2015; He et al. 2016; Huang et al. 2017) to effectively extract multi-scale features from RGB image and depth map. High-level features from deep layers represent coarse-scale and semantic information in an image, while low-level features from shallow layers capture fine-scale details for precisely localizing boundaries of objects. Due to this complementarity, effectively fusion information across scales is also a key to successful RGB-D saliency detection. In addition, CNN-based structures also contribute to the fusion of multi-scale multi-modal features. However, as a local operation, the receptive field of CNNs is limited by its kernel size and number of layers. It makes long-range dependency modeling difficult for feature fusion in saliency detection.

There have been several methods (Li, Liu, and Ling 2020; Gongyang et al. 2020; Piao et al. 2019; Chen and Li 2019, 2018) working on the fusion of multi-modal features across multiple scales with improved RGB-D saliency detection performance. However, most of them conduct feature fusion in a progressive manner by CNN-based local operations, that is, for each time, features from two modalities only fuse with each other within the same scale and at a local spatial neighborhood. This could cause insufficient integration of two modalities because the potential long-range dependencies would be restricted. In addition, these prior approaches tend to employ different techniques for different modules, *e.g.*, channel-wise concatenation or spatial attention for fusion across modalities; U-Net-like progressive integration for fusion across scales and recurrent attention for feature enhancement. Such diversity within modules leads to a potentially unwieldy complexity in the design of model architecture. This motivates us to design a uniform operation applied to multi-modal multi-scale fusion and even feature enhancement, which would simplify the model design and benefit performance boost of RGB-D saliency detection.

Inspired by transformer (Vaswani et al. 2017), a non-local model with self attention and cross attention layer to capture long-range dependencies in an image, we propose a novel transformer-based network for RGB-D saliency detection to address the aforementioned limitations. It contains a Transformer-based Feature Fusion Module (TFFM)

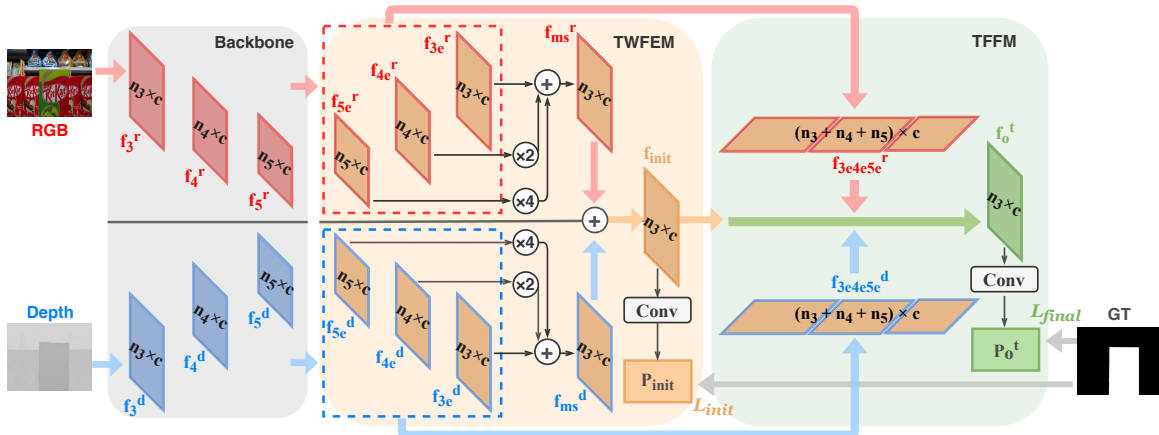


Figure 1: The structure of our overall method. Here, the $\times 2$, $\times 4$ in figure represent the $UP_{\times 2}(\cdot)$, $UP_{\times 4}(\cdot)$ in TWFEM.

to fuse multi-scale multi-modal features globally, and a Transformer-based Within-modality Feature Enhancement Module (TWFEM) to enhance features across scales within the same modality. Both of these modules are composed of only transformer decoders. And instead of only considering long-range dependencies among all positions within one feature, our proposed structure takes advantage of transformer’s non-local essence to simultaneously work on features among different modalities and multiple scales. For TFFM, in the self-attention layer of transformer, a guidance for global fusion is generated by refining an initial fused feature with its self-interaction between each two positions. In the cross-attention layer, features from different modalities and scales are taken as embeddings of a sequence. With such guidance, each position is equipped with a final fused feature that combines multi-modal and multi-scale information at all positions in the image, which is further fed to a classifier to predict the saliency probability map. In addition, TWFEM is employed within each modality to generate enhanced features fed to TFFM. It allows feature on each scale to look through features from all other scales at all positions to select and integrate complementary information for enhancement while remains its original resolution. It also simply produces the initial fused feature for TFFM. In this way, we are able to have a uniform design based on transformers for both feature enhancement and feature fusion, which simplify the model design and boost saliency detection performance.

Main contributions of this work are three-folded.

- We introduce a novel transformer-based framework for RGB-D saliency detection which simultaneously and globally integrates features across modalities and scales.

- Our RGB-D saliency detector uses only transformers as a uniform operations for both feature fusion and feature enhancement, which shows the potential of transformer in this task and simplifies the model design.

- Extensive experiments over six benchmark datasets show that the proposed transformer-based network generally performs favorably against state-of-the-art RGB-D saliency detection methods.

Related Work

RGB-D Saliency Detection

Early RGB-D saliency detection methods (Peng et al. 2014; Cheng et al. 2014; Zhu et al. 2017a; Cong et al. 2016; Zhu et al. 2017b; Zhu and Li 2017) focus on hand-crafted low-level features and thus struggled to handle complex scenes. More recent deep learning approaches extract high-level representations (Qu et al. 2017; Han et al. 2017) and obtain multi-scale features from different levels (Chen, Li, and Su 2019) to improve the performance. A common CNN architecture for RGB-D saliency detection involves a two-stream network to generate multi-scale features from two modalities, followed by several separate fusion processes via local operations. One approach (Li, Liu, and Ling 2020; Gongyang et al. 2020; Zhang et al. 2020b) first fuses multi-modal features separately within each scale and then combines the fused features across all scales. A second approach (Chen and Li 2018; Li et al. 2020; Pang et al. 2020) progressively merges the multi-modal features from coarse to fine scales. Generally these approaches rely on convolutional operations which allow only information from adjacent spatial positions to contribute to feature fusion at one time. To compensate for this limitation, some methods employ extra feature enhancement module. They design different structures for multi-scale feature fusion, multi-modal feature fusion and feature enhancement separately, which complicates the network and still fail to simultaneously consider long-term dependencies among all scales, modalities and positions. For example, Piao et al. (2019) use a recurrent module to enhance the fused features, while Liu, Zhang, and Han (2020) use attention to enhance features across modalities before fusion. Exceptions to the two-stream network approach do exist. Piao et al. (2020) use only RGB image as input to the single-stream network, and Zhao et al. (2020) use a single-stream network that combines the RGB and depth data directly from the input. But they also use a progressive approach for multi-scale fusion with local operations.

Transformers

The transformer model is first proposed by Vaswani et al. (2017) for the machine translation task. It has an encoder-decoder structure involving two kinds of attention. The

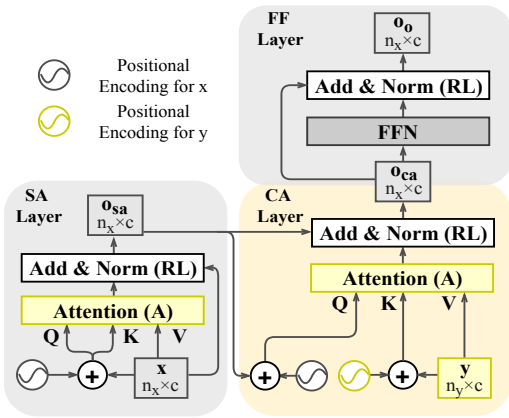


Figure 2: The structure of the transformer decoder module.

transformer encoder contains a self-attention layer, while the transformer decoder has both self-attention and cross-attention layers. The transformer model is adopted by Carion et al. (2020) to exploit non-local relationships for end-to-end object detection. A pixel-level feature extracted by a CNN-based backbone is refined by the self-attention layer in the transformer encoder module. The transformer decoder module then generates object-level feature from the refined encoder feature over all positions in an image. Zhu et al. (2020) and Zhang et al. (2020a) show that the transformer model is capable of using multi-scale pixel-level features simultaneously to achieve better performance for object detection and segmentation tasks. The transformer model is also used to transform multi-modal features for image caption and video retrieval (Li et al. 2019; Gabeur et al. 2020).

In this paper, we apply the structure of transformer to achieve simultaneous multi-modal and multi-scale feature fusion over all spatial positions for RGB-D saliency detection. We also show that transformer offers a unifying architecture which can also be applied for within-modality feature enhancement before fusion.

Method

In this section, we introduce the overall structure of our transformer-based network for RGB-D saliency detection. Both our transformer-based feature fusion module (TFFM) and transformer-based within-modality feature enhancement module (TWFEM) are based upon a common transformer decoder template. We review this template first, and then go into the specifics of the TFFM and TWFEM. The overall architecture is shown in Fig.1.

Transformer Decoder Module

The original transformer model (Vaswani et al. 2017) consists of a transformer encoder and a transformer decoder. Both of the TWFEM and TFFM only apply the structure of transformer decoder module. Here, we first introduce the attention module, the core of the transformer decoder module. Given a query $Q \in \mathbb{R}^{n_Q \times c}$, a key $K \in \mathbb{R}^{n_P \times c}$, and a value $V \in \mathbb{R}^{n_P \times c}$, the dot-product attention A is computed to output a weighted sum of V , with weights given by a compatibility function of Q with K (Shen et al. 2021):

$$A(Q, K, V) = \rho(QK^T)V \quad (1)$$

Here n_Q is the number of positions in feature Q . K, V share the same number of positions n_P . c is the common feature dimensionality for Q, K, V . $\rho(\cdot)$ represents the softmax function along each row (see (Shen et al. 2021; Vaswani et al. 2017) for details). The output of this attention module has the same size $\mathbb{R}^{n_Q \times c}$ as Q .

In this paper, we follow Vaswani et al. (2017) and apply the same structure of transformer decoder module. Transformer decoder requires two input features: $x \in \mathbb{R}^{n_x \times c}$ and $y \in \mathbb{R}^{n_y \times c}$. It is able to refine x by selecting and integrating relevant information from y based on the global relationship between x and y over all positions. It is implemented by three sub-layers: a self-attention (SA) layer, a cross-attention (CA) layer and a feedforward (FF) layer. Both self-attention and cross-attention layers contain an attention module (A) and a Residual connection and Layer normalization block (RL). Feedforward layer contains a feedforward network (FFN) with two linear transformations and a ReLU activation in between, and a RL block.

$$\begin{aligned} o_{sa} &= SA(x) = RL(A(\tilde{x}, \tilde{x}, x)) \\ o_{ca} &= CA(o_{sa}, y) = RL(A(\tilde{o}_{sa}, \tilde{y}, y)) \\ o_o &= FF(o_{ca}) = RL(FFN(o_{ca})) \end{aligned} \quad (2)$$

$o_{sa}, o_{ca}, o_o \in \mathbb{R}^{n_x \times c}$ are the outputs of self-attention, cross-attention, feedforward layers and have the same size with input x . For each attention module, Q and K are added by their corresponding positional encodings as (Carion et al. 2020) and represented as $\tilde{x}, \tilde{o}_{sa}, \tilde{y}$. It help to consider the spatial information between any two positions in Q and K for learning the attention weight, which is essential especially when Q and K have different number of positions. Here, the self-attention layer uses x as Q, K, V in attention module, which refines x based on its self-relationship between any two positions to achieve a better query o_{sa} for the cross-attention layer. The cross-attention layer uses o_{sa} as Q and y as K, V in attention module, which looks through all positions of y to extract useful information for o_{sa} to get its further refined feature o_{ca} . The final output o_o is then calculated from o_{ca} by feedforward layer. We can name the above processes as one transformer decoder block (TD) and have $o_o = TD(x, y)$. The meanings of x and y are specified in TFFM and TWFEM. And we show the overall structure of transformer decoder in Fig.2.

To save the memory and computational costs, we employ an efficient attention implementation (Shen et al. 2021) to replace the original attention module (A) in transformer decoder module. Instead of multiplying Q and K first to form an $n_Q \times n_P$ matrix, Efficient attention (EA) first multiples K^T and V to form a $c \times c$ matrix:

$$EA(Q, K, V) = \rho_q(Q)(\rho_k(K)^T V) \quad (3)$$

where $\rho_q(\cdot)$ and $\rho_k(\cdot)$ are the softmax function along each row of Q and each column of K respectively. Since c is normally much smaller than the number of positions $n = h \times w$, h, w are the height and width for feature, it efficiently decreases the computational costs and still aggregates value features from all positions in a global way. Besides, the efficient attention we employ also has the function of multi-head as (Vaswani et al. 2017).

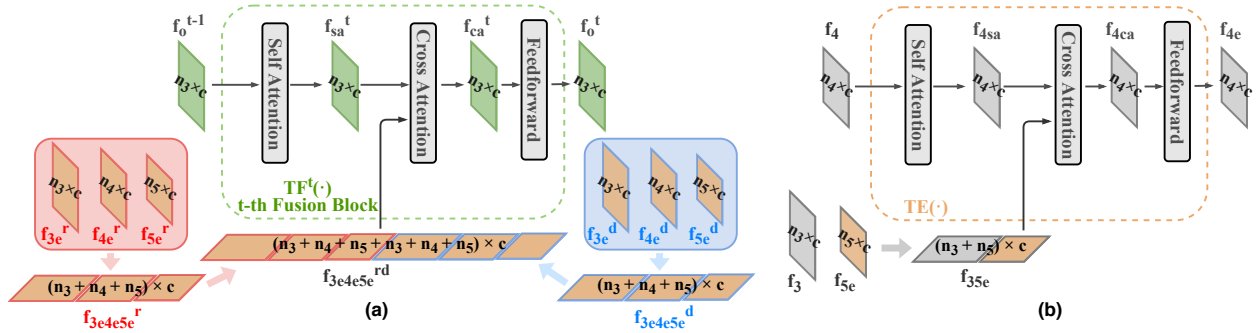


Figure 3: (a) The structure of our t -th transformer-based feature fusion block $TF^t(\cdot)$ (Eq. 5). (b) The structure of our transformer-based feature enhancement block $TE(\cdot)$, we use the process of generating the enhanced f_{4e} (Eq. 9) as example.

Transformer-based Feature Fusion Module

We apply a common two-stream network as existing RGB-D saliency detection methods (Piao et al. 2019; Zhang et al. 2020b) where each stream uses VGG16 (Simonyan and Zisserman 2015) as backbone to extract three-scale features for one modality. Therefore, how to automatically fuse multi-modal multi-scale features becomes the key to RGB-D saliency detection. Different from most of the previous attempts that separately process multi-modal fusion and multi-scale fusion via local operations, we propose a transformer-based feature fusion module (TFFM). It manages to simultaneously fuse multi-scale multi-modal features in a global way, where the fused feature at each positions is calculated by a adaptively weighted combination of information from all features at all positions. Following (Carion et al. 2020), our TFFM also contains several fusion blocks which manage to refine the fused feature gradually.

We apply the structure of transformer decoder for each fusion block. As mentioned above, the transformer decoder module requires two inputs, x and y , it selects useful information from y to refine x . For our global feature fusion, input y should contains information from all scales and modalities. We obtain and denote features of three scales from RGB and depth streams as $f_{ie}^r \in \mathbb{R}^{n_i \times c}$ and $f_{ie}^d \in \mathbb{R}^{n_i \times c}$ respectively (see TWFEM), where $i \in \{3, 4, 5\}$, $n_i = h_i \times w_i$. Note that these multi-scale features have different n_i , h_i , w_i but share the the same dimensionality c . We do not need to upsample all these features to the same size to fuse features with different resolutions together. Instead, we directly concatenate $\{f_{3e}, f_{4e}, f_{5e}\}^r$ for RGB stream to get $f_{3e4e5e}^r \in \mathbb{R}^{n_{345} \times c}$, where $n_{345} = n_3 + n_4 + n_5$, and $\{f_{3e}, f_{4e}, f_{5e}\}^d$ for depth stream to get $f_{3e4e5e}^d \in \mathbb{R}^{n_{345} \times c}$. This practice is more suitable for our TFFM for two reasons. Firstly, in each fusion block, we need to have access to all multi-scale multi-modal features. Upsampling these features to a higher resolution when using them repeatedly increases the memory and computational costs, while our processing would save these resources by remaining features to their original sizes. Secondly, objects in a scene have large variations in scales. By maintaining multi-scale features to their original resolutions, our method manage to cover objects over all scales since features in lower resolution will still help predict objects with larger sizes, while features in higher resolution will continue detecting small objects and boundaries. After that, we concatenate two-stream features f_{3e4e5e}^r and f_{3e4e5e}^d

together as $f_{3e4e5e}^{rd} \in \mathbb{R}^{(n_{345} \times 2) \times c}$. f_{3e4e5e}^{rd} is used as y to provide abundant information from all scales and modalities.

Input x for each fusion block is a guidance of global feature fusion and have the same size with the output fused feature. Carion et al. (2020) use a stack of transformer decoder blocks to generate object-level feature from pixel-level feature, its x should have the same size with the output object-level feature. However, since there is no object-level prior information, x for its first block has to be set as a zero tensor so that the object-level feature has to be generated from zero. While for our RGB-D saliency detection, an initial fused feature $f_{init} \in \mathbb{R}^{n_3 \times c}$ with a higher resolution can be easily obtained (see TWFEM) and used as x in the first fusion block to provide a better guidance for feature fusion. With the required f_{init} and f_{3e4e5e}^{rd} , the overall process of the first transformer-based fusion block is as follows:

$$\begin{aligned} f_{sa} &= SA(f_{init}) \\ f_{ca} &= CA(f_{sa}, f_{3e4e5e}^{rd}) \\ f_o &= FF(f_{ca}) \end{aligned} \quad (4)$$

With f_{init} as query, we first apply a self-attention layer to refine itself for achieving a better guidance f_{sa} for fusion. And then in the cross-attention layer, f_{sa} on each position is refined by looking through all positions in f_{3e4e5e}^{rd} to generate a better fused feature f_{ca} . Therefore, for each positions in f_{ca} , it contains information which is adaptively selected and fused from all positions in multi-scale multi-modal features. The feedforward layer is applied to get the output fused feature $f_o \in \mathbb{R}^{n_3 \times c}$ which has the same size as f_{init} . Note that the positional encoding of f_{3e4e5e}^{rd} is obtained by concatenating positional encodings of all multi-scale multi-modal features in sequence. Even though features in f_{3e4e5e}^{rd} have different resolutions, this transformer-based block would still consider the spatial information during fusion.

In the following fusion blocks, input x is replaced by the output f_o from a previous block. We name this transformer-based fusion block as TF and the process of t -th fusion block can be written as:

$$f_o^t = TF^t(f_o^{t-1}, f_{3e4e5e}^{rd}) \quad (5)$$

where $t \in [1, \dots, T]$, T denotes the number of the straight-forward fusion blocks in our TFFM. f_o^t is the output of t -th block. $f_o^0 = f_{init}$ is the input x for the first block, $TF^t(\cdot)$ represents the process in t -th fusion block.

The proposed TFFM manages to fuse multi-scale multi-modal simultaneously in a global way. Meanwhile, by using several fusion blocks, our method is able to generate the final fused feature gradually with information from all scales, modalities and positions. The architecture of one transformer-based feature fusion block is shown in Fig.3 (a).

With $f_o^t \in \mathbb{R}^{n_3 \times c}$ output from each block, it is first reshaped back to form $\mathbb{R}^{c \times h_3 \times w_3}$. Then it is used to obtain saliency prediction P_o^t by one convolutional layer as a classifier. For better supervision on all the fusion processes in all T fusion blocks, f_o^t from all blocks are used to produce T saliency maps. The overall prediction loss is calculated by:

$$\mathcal{L}_{final} = \sum_{t=1}^T \mathcal{L}_{bce}(P_o^t, S) \quad (6)$$

where \mathcal{L}_{bce} stands for the binary cross-entropy loss, S is the saliency ground-truth. And the convolutional layer is shared among all T blocks for predicting the saliency maps from all T fused features.

Transformer-based Within-modality Feature Enhancement Module

To further improve the performance, a TWFEM is proposed to generate the enhanced multi-scale features $\{f_{3e}, f_{4e}, f_{5e}\}$ for each modality separately and a simple initial fused feature f_{init} before TFFM. Firstly, feature on each scale are enhanced by further extracting and integrating complementary information from other scales within the same modality while remains its original resolution. It is also implemented as stacks of transformer decoders which indicates the flexibility of transformer decoder and uniformity of the proposed framework. Secondly, f_{init} is computed by simply fusing enhanced multi-scale features of two modalities. It is used in TFFM as a better guidance for global feature fusion.

We first show how to generate $\{f_{3e}, f_{4e}, f_{5e}\}$ for each modality separately. For each stream, we can directly extract three-scale features from its backbone network separately and apply one convolution layer for each feature to make them have the same dimensionality c , which are denoted as $f_i^r \in \mathbb{R}^{c \times h_i \times w_i}$ and $f_i^d \in \mathbb{R}^{c \times h_i \times w_i}$ for features from RGB stream and depth stream, where $i \in \{3, 4, 5\}$. This is a simple way to extract the feature on each scale for each modality, while these features can be further enhanced by automatically selecting and integrating complementary information from other scales since features with different scales contain different levels of information. Features from coarser scales contain more semantic information, while features from finer scales contain more detailed information. Therefore, the structure of transformer decoder is suitable for feature enhancement across scales. It allows the enhanced features to contain richer information from different scales while remain their original resolutions.

We reshape all features to form $f_i \in \mathbb{R}^{n_i \times c}$ and then enhance features within the same modality from coarse scale to fine scale in a progressive way. It also uses the structure of transformer decoder. For each f_i , we enhance it by setting itself as input x , the concatenation of features from its finer scales (f_j where $j > i, j \in [3, 4, 5]$) and the enhanced features from its coarser scales (f_{le} where $l < i, l \in [3, 4, 5]$)

as input y . It means for each stream, we first enhance the coarsest-scale feature f_5 by f_3, f_4 from the same modality while remaining f_5 's original resolution. The enhancement process consists of a self-attention layer to refine f_5 by itself, a cross-attention layer to extract and integrate complementary information from f_3, f_4 , and a feedforward layer:

$$\begin{aligned} f_{5sa} &= SA(f_5) \\ f_{5ca} &= CA(f_{5sa}, f_{34}) \\ f_{5e} &= FF(f_{5ca}) \end{aligned} \quad (7)$$

where $f_{34} \in \mathbb{R}^{(n_3+n_4) \times c}$ is formed by concatenating f_3 and f_4 . $f_{5e} \in \mathbb{R}^{n_5 \times c}$ is the enhanced feature of f_5 . Here, we also select and integrate useful information in a global way where features from all spatial positions in f_3 and f_4 can be contributed to each position in f_{5e} . We name it as a transformer-based enhancement block (TE) and the above process for enhancing f_5 can be represented as:

$$f_{5e} = TE(f_5, f_{34}) \quad (8)$$

Similarly, we can progressively compute enhanced features for the other two scales. For f_{4e} , its complementary information is extracted from f_3 and the enhanced f_{5e} for integration, and for f_{3e} , it is from the enhanced f_{4e} and f_{5e} :

$$f_{4e} = TE(f_4, f_{35e}) \quad (9)$$

$$f_{3e} = TE(f_3, f_{4e5e}) \quad (10)$$

where $f_{35e} \in \mathbb{R}^{(n_3+n_5) \times c}$ is the concatenation of f_3 and f_{5e} . $f_{4e5e} \in \mathbb{R}^{(n_4+n_5) \times c}$ is the concatenation of f_{4e} and f_{5e} . The structure of our $TE(\cdot)$ is shown in Fig.3 (b).

Then, with the enhanced feature $f_{ie} \in \mathbb{R}^{n_i \times c}$, $i \in \{3, 4, 5\}$ from both two modalities, we start to generate the simple initial fused feature f_{init} by a simple way to first fuse multi-scale features by addition for each modality, then fuse multi-modal features:

$$\begin{aligned} f_{ms} &= f_{3e} + UP_{\times 2}(f_{4e}) + UP_{\times 4}(f_{5e}) \\ f_{init} &= f_{ms}^r + f_{ms}^d \end{aligned} \quad (11)$$

where $UP_{\times 2}(\cdot), UP_{\times 4}(\cdot)$ stand for $\times 2, \times 4$ upsample function, which first reshape f_{ie} to form $\mathbb{R}^{c \times h_i \times w_i}$, then apply the corresponding bilinear upsampling and reshape it back to form $\mathbb{R}^{n_3 \times c}$ as f_{3e} . For getting a better guidance for TFFM, we reshape f_{init} back to form $\mathbb{R}^{c \times h_3 \times w_3}$ and apply one convolutional layer on it as a classifier to get an initial saliency prediction map P_{init} . P_{init} can be supervised by the saliency ground-truth S :

$$\mathcal{L}_{init} = \mathcal{L}_{bce}(P_{init}, S) \quad (12)$$

Experiments

Datasets and Evaluation Metrics

We evaluate our proposed method on six widely used RGB-D saliency datasets including NJUD (Ju et al. 2014), NLPR (Peng et al. 2014), STERE (Niu et al. 2012), DES (Cheng et al. 2014), SIP (Fan et al. 2019), and DUT-D (Piao et al. 2019). Following Piao et al. (2019), we use the selected 800 images from DUT-D, 1485 images from NJUD and 700 images from NLPR for training our network. We

Table 1: Results on different datasets. We highlight the best three results in each column in **bold**, **bold** and *underline*.

Dataset	Metric	CPFP	DMRA	ICNet	DANet	CMWNet	S2MA	A2dele	PGAR	SSF	HDFNet	Ours
DES	MAE	0.038	0.030	0.027	0.028	0.022	<u>0.021</u>	0.029	0.026	0.026	0.020	0.018
	F_m	0.829	0.867	0.889	0.891	0.900	<u>0.906</u>	0.868	0.880	0.883	0.919	0.921
	S_m	0.872	0.899	0.920	0.905	<u>0.934</u>	0.941	0.883	0.913	0.903	0.932	0.932
	E_m	0.927	0.944	0.959	0.961	0.967	0.974	0.919	0.939	0.946	<u>0.973</u>	0.975
DUT-D	MAE	0.100	0.048	0.072	0.047	0.056	0.044	0.042	<u>0.035</u>	0.034	0.040	0.030
	F_m	0.735	0.883	0.830	0.884	0.866	0.885	0.891	0.914	0.914	<u>0.892</u>	0.923
	S_m	0.749	0.887	0.852	0.889	0.887	0.902	0.884	0.919	<u>0.914</u>	0.905	0.924
	E_m	0.815	0.930	0.901	0.929	0.922	0.935	0.929	<u>0.950</u>	0.951	0.938	0.954
NJUD	MAE	0.053	0.051	0.052	0.046	0.046	0.053	0.051	<u>0.042</u>	0.043	0.037	0.036
	F_m	0.837	0.872	0.868	0.877	0.880	0.865	0.873	0.893	<u>0.885</u>	0.894	0.894
	S_m	0.878	0.885	0.894	0.897	0.903	0.894	0.868	<u>0.909</u>	0.898	<u>0.911</u>	0.913
	E_m	0.900	0.920	0.913	0.926	0.923	0.916	0.916	0.935	<u>0.934</u>	<u>0.934</u>	0.932
NLPR	MAE	0.038	0.031	0.028	0.031	0.029	0.030	0.028	0.024	0.026	<u>0.027</u>	0.024
	F_m	0.818	0.855	0.870	0.865	0.859	0.853	<u>0.878</u>	0.885	0.875	<u>0.878</u>	0.895
	S_m	0.884	0.898	0.922	0.908	<u>0.917</u>	0.915	0.895	0.930	0.913	0.916	<u>0.924</u>
	E_m	0.920	0.942	0.945	0.945	0.940	0.942	0.945	0.955	0.951	<u>0.948</u>	0.960
SIP	MAE	0.064	0.088	0.069	<u>0.054</u>	0.062	0.057	0.070	0.055	0.057	0.050	0.049
	F_m	0.819	0.815	0.836	0.864	0.851	0.854	0.829	0.854	0.850	<u>0.863</u>	0.866
	S_m	0.850	0.800	0.854	0.878	0.867	0.872	0.826	<u>0.876</u>	0.867	0.878	0.885
	E_m	0.899	0.858	0.900	<u>0.917</u>	0.909	0.913	0.889	0.912	0.913	0.920	0.921
STERE	MAE	0.051	0.050	0.045	0.047	0.043	0.051	0.044	0.041	0.044	<u>0.039</u>	<u>0.042</u>
	F_m	0.830	0.869	0.865	0.858	0.869	0.855	<u>0.877</u>	0.880	0.862	0.879	0.880
	S_m	0.879	0.874	0.902	0.892	<u>0.905</u>	0.890	0.876	0.907	0.889	0.906	0.901
	E_m	0.907	0.926	0.926	0.926	<u>0.930</u>	0.926	0.928	0.937	0.927	0.937	0.934
Model Size (MB)		291.9	238.8	312.2	106.8	342.9	346.8	60.1	64.9	131.8	176.9	129.9

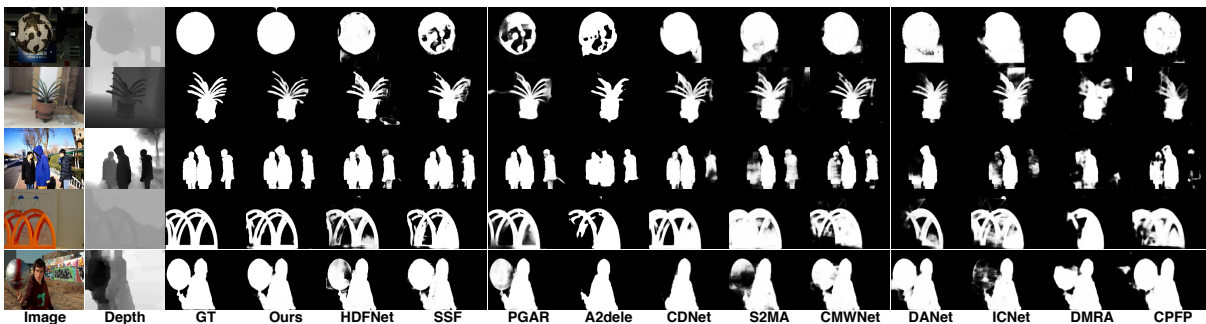


Figure 4: Visual comparison between our method and the state-of-the-art methods.

then evaluate our model on the remaining images in these three datasets and the other three datasets.

We adopt four widely used evaluation metrics for quantitative evaluation including F-measure (F_m) (Achanta et al. 2009), mean absolute error (MAE) (Borji et al. 2015), S-measure (S_m) (Fan et al. 2017) and E-measure (E_m) (Fan et al. 2018). In this paper, we report the mean F-measure value with the adaptive threshold as F_m . For MAE, the lower value means the method is better, while for all other metrics, the higher value means the method is better.

Implementation Details

We apply PyTorch toolbox for implementation using one GeForce RTX 2080Ti GPU with 11 GB memory. The parameters of two-stream backbone networks are both initialized by VGG16 (Simonyan and Zisserman 2015). The input RGB images and depth images are all resized to 256×256 . We train our method for 150k iterations by ADAM optimizer (Kingma and Ba 2015). The initial learning rate, batch size, number of channel c and number of blocks T in TFFM are set to $1e-4$, 6, 128 and 4. During evaluation, the output prediction map of the last transformer-based fusion block is

used as the final saliency prediction map.

Comparison with state-of-the-art methods

To verify the effectiveness of our proposed transformer-based network for RGB-D saliency detection, we compare our performance and model size with ten state-of-art RGB-D saliency detection methods including: DANet (Zhao et al. 2020), SSF (Zhang et al. 2020b), S2MA (Liu, Zhang, and Han 2020), ICNET (Li, Liu, and Ling 2020), CMWNet (Gongyang et al. 2020), DMRA (Piao et al. 2019), CPFP (Zhao et al. 2019), A2dele (Piao et al. 2020), PGAR (Chen and Fu 2020), and HDFNet (Pang et al. 2020) in Table 1. For a fair comparison, we report the results and model sizes with VGG16 as backbone for DANet and HDFNet.

It demonstrates that our proposed transformer-based network generally performs favorably against all the listed state-of-the-art methods. It benefits from our TFFM which requires a global and adaptive response of information from all scales, all modalities and all spatial positions for our final fused feature at each position, and our TWFEM which enhances feature on each scale with complementary infor-

Table 2: Ablation study on our proposed transformer-based network. We highlight the best result in each column in **bold**.

Index	MSMMF	model		STERE				NLPR				DUT-D			
		TWFEM	TFFM	MAE	F_m	S_m	E_m	MAE	F_m	S_m	E_m	MAE	F_m	S_m	E_m
1	✓			0.054	0.846	0.865	0.915	0.031	0.863	0.901	0.945	0.045	0.889	0.891	0.932
2	✓	✓		0.045	0.861	0.888	0.925	0.028	0.877	0.913	0.950	0.037	0.901	0.908	0.942
3	✓		✓	0.043	0.876	0.894	0.931	0.027	0.888	0.916	0.953	0.035	0.912	0.914	0.949
4	✓	w/o prog		0.042	0.873	0.901	0.930	0.025	0.887	0.922	0.955	0.032	0.913	0.921	0.948
5	✓	✓	✓	0.042	0.880	0.901	0.934	0.024	0.895	0.924	0.960	0.030	0.923	0.924	0.954

Table 3: Comparison of setting different T for the entangled architecture. We highlight the best result in each column in **bold**.

model	STERE				NLPR				DUT-D			
	MAE	F_m	S_m	E_m	MAE	F_m	S_m	E_m	MAE	F_m	S_m	E_m
T = 0	0.045	0.861	0.888	0.925	0.028	0.877	0.913	0.950	0.037	0.901	0.908	0.942
T = 2	0.041	0.876	0.900	0.933	0.025	0.884	0.920	0.952	0.031	0.917	0.920	0.951
T = 4	0.042	0.880	0.901	0.934	0.024	0.895	0.924	0.960	0.030	0.923	0.924	0.954
T = 5	0.040	0.880	0.905	0.934	0.025	0.891	0.921	0.956	0.029	0.923	0.926	0.956

mation from other scales within the same modality.

Moreover, since we only use the transformer-based structure with the efficient attention for both feature fusion and enhancement instead of designing diverse and complicated structures, the model size of our network is smaller than almost all the other two-stream methods except for PGAR. It is because PGAR uses a much lighter network as backbone than VGG16 for depth stream which only contains four convolution layers. Our model size is also larger than A2dele and DANet since they apply the one-stream network. A2dele only has RGB image as input and DANet combines RGB images and depth maps together as one input of one-stream network. We also present some qualitative examples in Fig.4. It shows that our method not only precisely predicts the whole saliency objects (e.g. row 1), but also accurately detects the boundaries of saliency regions (e.g. row 4).

Ablation Study

Effectiveness of each transformer-based module. To demonstrate the impact of each part in our overall network, we conduct ablation studies by evaluating five subset-models and present results on three RGB-D datasets. As shown in Table 2, model 1 which only uses MSMMF means a simple multi-scale multi-modal fusion method using Eq.11 in which f_{ie} is replaced by f_i since we do not have the enhanced features. And the following models add TWFEM and TFFM separately to see the impact of each transformer-based module. Model 5 is our overall performance by using both TWFEM and TFFM. For model 4, we also use both TWFEM and TFFM, but in its TWFEM, we do not use the progressive way to get enhanced features f_{4e} and f_{3e} as in Eq.9, Eq.10. Instead, we directly use f_3, f_5 to get f_{4e} and f_4, f_5 to get f_{3e} . We show the impact of our progressive enhanced way by the comparison between model 4 and model 5. We also include some visual examples in Fig.5.

It indicates that for model 1 which only fuses multi-scale and multi-modal features in a simple way for saliency prediction may perform well on some simple situations. However, without a global and adaptive fusion, it is not suit-

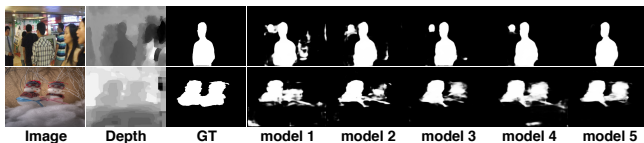


Figure 5: Visual examples for ablation study.

able for complex scenes which causes poor performance on datasets like STERE. Our TFFM can significantly improve the performance since it allows this global and adaptive fusion, which also improves the ability of generalization for complex situations. Our TWFEM enhances features with complimentary information across scales which not only gains improvements for model 2 with only a simple fusion, but also provides features with more abundant information for TFFM. We also show that the progressively enhanced feature from coarse to fine scale in our TWFEM can provide further improvements for saliency prediction.

Effectiveness of T. We also discuss the chosen number of blocks in our TFFM by conducting the experiments to set $T = 0, 2, 4, 5$ for the fusion blocks in our overall transformer-based network (by setting $T = 0$ is equal to model 2 in Table 2). We present the comparisons on three datasets in Table 3. Since the initial fused feature from our TWFEM provides useful information related to saliency prediction for our TFFM as the initial guidance. By setting different T may not have a significant influence on the final result predicted by the output feature from the last block, especially when T is large enough. However, using a small number of blocks may still affect the performance on some datasets such as the NLPR dataset. Considering both the performance and the efficiency of our model, we choose $T = 4$ for our transformer-based network.

Conclusion

In this paper, we propose a transformer-based network for RGB-D saliency detection, which uses transformer as a uniform operation for both feature enhancement and feature fusion. It consists of two stages: Firstly, a transformer-based single-modal feature enhancement module (TWFEM) enhances feature on each scale by selecting and integrating complementary information from other scales within the same modality. It also generates a simple initial fused feature. Secondly, our transformer-based fusion module (TFFM) uses the initial fused feature as a guidance to simultaneously fuse multi-scale, multi-modal features. It generates a final fused feature that at each position, calculates by an adaptive combination of information from all scales and both modalities which captures the long-range dependencies. Evaluation results on six RGB-D datasets demonstrate the effectiveness of our method by performing favorably against state-of-the-art RGB-D saliency methods.

References

- Achanta, R.; Hemami, S.; Estrada, F.; and Susstrunk, S. 2009. Frequency-tuned Saliency Region Detection. In *2009 IEEE Conference on Computer Vision and Pattern Recognition*, 1597–1604. IEEE.
- Borji, A.; Cheng, M.-M.; Jiang, H.; and Li, J. 2015. Saliency Object Detection: A Benchmark. *IEEE Transactions on Image Processing*, 24(12): 5706–5722.
- Carion, N.; Massa, F.; Synnaeve, G.; Usunier, N.; Kirillov, A.; and Zagoruyko, S. 2020. End-to-end Object Detection with Transformers. In *European Conference on Computer Vision*, 213–229. Springer.
- Chen, H.; and Li, Y. 2018. Progressively Complementarity-aware Fusion Network for RGB-D Saliency Object Detection. In *Proceedings of the IEEE conference on computer vision and pattern recognition*, 3051–3060.
- Chen, H.; and Li, Y. 2019. Three-stream Attention-aware Network for RGB-D Saliency Object Detection. *IEEE Transactions on Image Processing*, 28(6): 2825–2835.
- Chen, H.; Li, Y.; and Su, D. 2019. Multi-modal Fusion Network with Multi-scale Multi-path and Cross-modal Interactions for RGB-D Saliency Object Detection. *Pattern Recognition*, 86: 376–385.
- Chen, S.; and Fu, Y. 2020. Progressively Guided Alternate Refinement Network for RGB-D Saliency Object Detection. In *European Conference on Computer Vision*, 520–538. Springer.
- Cheng, Y.; Fu, H.; Wei, X.; Xiao, J.; and Cao, X. 2014. Depth Enhanced Saliency Detection Method. In *Proceedings of international conference on internet multimedia computing and service*, 23–27.
- Cong, R.; Lei, J.; Zhang, C.; Huang, Q.; Cao, X.; and Hou, C. 2016. Saliency Detection for Stereoscopic Images Based on Depth Confidence Analysis and Multiple Cues Fusion. *IEEE Signal Processing Letters*, 23(6): 819–823.
- Fan, D.-P.; Cheng, M.-M.; Liu, Y.; Li, T.; and Borji, A. 2017. Structure-measure: A New Way to Evaluate Foreground Maps. In *Proceedings of the IEEE International Conference on Computer Vision*, 4548–4557.
- Fan, D.-P.; Gong, C.; Cao, Y.; Ren, B.; Cheng, M.-M.; and Borji, A. 2018. Enhanced-alignment Measure for Binary Foreground Map Evaluation. *arXiv preprint arXiv:1805.10421*.
- Fan, D.-P.; Lin, Z.; Zhao, J.-X.; Liu, Y.; Zhang, Z.; Hou, Q.; Zhu, M.; and Cheng, M.-M. 2019. Rethinking RGB-D Saliency Object Detection: Models, Datasets, and Large-scale Benchmarks. *arXiv preprint arXiv:1907.06781*.
- Gabeur, V.; Sun, C.; Alahari, K.; and Schmid, C. 2020. Multi-modal Transformer for Video Retrieval. In *European Conference on Computer Vision (ECCV)*, volume 5. Springer.
- Gongyang, L.; Zhi, L.; Linwei, Y.; Yang, W.; and Haibin, L. 2020. Cross-modal Weighting Network for RGB-D Saliency Object Detection. In *European Conference on Computer Vision*. Springer.
- Han, J.; Chen, H.; Liu, N.; Yan, C.; and Li, X. 2017. CNNs-based RGB-D Saliency Detection via Cross-view Transfer and Multiview Fusion. *IEEE transactions on cybernetics*, 48(11): 3171–3183.
- He, J.; Feng, J.; Liu, X.; Cheng, T.; Lin, T.-H.; Chung, H.; and Chang, S.-F. 2012. Mobile Product Search with Bag of Hash Bits and Boundary Reranking. In *2012 IEEE Conference on Computer Vision and Pattern Recognition*, 3005–3012. IEEE.
- He, K.; Zhang, X.; Ren, S.; and Sun, J. 2016. Deep Residual Learning for Image Recognition. In *Proceedings of the IEEE Conference on Computer Vision and Pattern Recognition*, 770–778.
- Huang, G.; Liu, Z.; Van Der Maaten, L.; and Weinberger, K. Q. 2017. Densely Connected Convolutional Networks. In *Proceedings of the IEEE Conference on Computer Vision and Pattern Recognition*, 4700–4708.
- Ju, R.; Ge, L.; Geng, W.; Ren, T.; and Wu, G. 2014. Depth Saliency based on Anisotropic Center-surround Difference. In *2014 IEEE International Conference on Image Processing (ICIP)*, 1115–1119. IEEE.
- Kingma, D. P.; and Ba, J. 2015. Adam: A Method for Stochastic Optimization. In *ICLR*.
- Lee, H.; and Kim, D. 2018. Saliency Region-based Online Object Tracking. In *2018 IEEE Winter Conference on Applications of Computer Vision (WACV)*, 1170–1177. IEEE.
- Li, C.; Cong, R.; Piao, Y.; Xu, Q.; and Loy, C. C. 2020. RGB-D Saliency Object Detection with Cross-modality Modulation and Selection. In *European Conference on Computer Vision*, 225–241. Springer.
- Li, G.; Liu, Z.; and Ling, H. 2020. ICNet: Information Conversion Network for RGB-D based Saliency Object Detection. *IEEE Transactions on Image Processing*, 29: 4873–4884.
- Li, G.; Zhu, L.; Liu, P.; and Yang, Y. 2019. Entangled Transformer for Image Captioning. In *Proceedings of the IEEE/CVF International Conference on Computer Vision*, 8928–8937.
- Liu, N.; Zhang, N.; and Han, J. 2020. Learning Selective Self-mutual Attention for RGB-D Saliency Detection. In *Proceedings of the IEEE/CVF Conference on Computer Vision and Pattern Recognition*, 13756–13765.
- Niu, Y.; Geng, Y.; Li, X.; and Liu, F. 2012. Leveraging Stereopsis for Saliency Analysis. In *2012 IEEE Conference on Computer Vision and Pattern Recognition*, 454–461. IEEE.
- Pang, Y.; Zhang, L.; Zhao, X.; and Lu, H. 2020. Hierarchical Dynamic Filtering Network for RGB-D Saliency Object Detection. In *Computer Vision—ECCV 2020: 16th European Conference, Glasgow, UK, August 23–28, 2020, Proceedings, Part XXV 16*, 235–252. Springer.
- Peng, H.; Li, B.; Xiong, W.; Hu, W.; and Ji, R. 2014. RGBD Saliency Object Detection: A Benchmark and Algorithms. In *European Conference on Computer Vision*, 92–109. Springer.
- Piao, Y.; Ji, W.; Li, J.; Zhang, M.; and Lu, H. 2019. Depth-Induced Multi-Scale Recurrent Attention Network for Saliency Detection. In *Proceedings of the IEEE International Conference on Computer Vision*, 7254–7263.

- Piao, Y.; Rong, Z.; Zhang, M.; Ren, W.; and Lu, H. 2020. A2dele: Adaptive and Attentive Depth Distiller for Efficient RGB-D Saliency Object Detection. In *Proceedings of the IEEE/CVF Conference on Computer Vision and Pattern Recognition*, 9060–9069.
- Qu, L.; He, S.; Zhang, J.; Tian, J.; Tang, Y.; and Yang, Q. 2017. RGBD Saliency Object Detection via Deep Fusion. *IEEE Transactions on Image Processing*, 26(5): 2274–2285.
- Shen, Z.; Zhang, M.; Zhao, H.; Yi, S.; and Li, H. 2021. Efficient Attention: Attention with Linear Complexities. In *Proceedings of the IEEE/CVF Winter Conference on Applications of Computer Vision*, 3531–3539.
- Simonyan, K.; and Zisserman, A. 2015. Very Deep Convolutional Networks for Large-scale Image Recognition. In *ICLR*.
- Vaswani, A.; Shazeer, N.; Parmar, N.; Uszkoreit, J.; Jones, L.; Gomez, A. N.; Kaiser, Ł.; and Polosukhin, I. 2017. Attention is All You Need. In *Advances in Neural Information Processing Systems*, 5998–6008.
- Wang, W.; Shen, J.; and Ling, H. 2018. A Deep Network Solution for Attention and Aesthetics Aware Photo Cropping. *IEEE Transactions on Pattern Analysis and Machine Intelligence*, 41(7): 1531–1544.
- Xu, K.; Ba, J.; Kiros, R.; Cho, K.; Courville, A.; Salakhudinov, R.; Zemel, R.; and Bengio, Y. 2015. Show, Attend and Tell: Neural Image Caption Generation with Visual Attention. In *International Conference on Machine Learning*, 2048–2057.
- Zhang, D.; Zhang, H.; Tang, J.; Wang, M.; Hua, X.; and Sun, Q. 2020a. Feature Pyramid Transformer. In *European Conference on Computer Vision*, 323–339. Springer.
- Zhang, M.; Ren, W.; Piao, Y.; Rong, Z.; and Lu, H. 2020b. Select, Supplement and Focus for RGB-D Saliency Detection. In *Proceedings of the IEEE/CVF Conference on Computer Vision and Pattern Recognition*, 3472–3481.
- Zhao, J.-X.; Cao, Y.; Fan, D.-P.; Cheng, M.-M.; Li, X.-Y.; and Zhang, L. 2019. Contrast Prior and Fluid Pyramid Integration for RGBD Saliency Object Detection. In *Proceedings of the IEEE Conference on Computer Vision and Pattern Recognition*, 3927–3936.
- Zhao, X.; Zhang, L.; Pang, Y.; Lu, H.; and Zhang, L. 2020. A Single Stream Network for Robust and Real-time RGB-D Saliency Object Detection. In *European Conference on Computer Vision*, 646–662. Springer.
- Zhu, C.; and Li, G. 2017. A Three-pathway Psychobiological Framework of Saliency Object Detection using Stereoscopic Technology. In *Proceedings of the IEEE International Conference on Computer Vision Workshops*, 3008–3014.
- Zhu, C.; Li, G.; Guo, X.; Wang, W.; and Wang, R. 2017a. A Multilayer Backpropagation Saliency Detection Algorithm based on Depth Mining. In *International Conference on Computer Analysis of Images and Patterns*, 14–23. Springer.
- Zhu, C.; Li, G.; Wang, W.; and Wang, R. 2017b. An Innovative Saliency Object Detection using Center-dark Channel Prior. In *Proceedings of the IEEE International Conference on Computer Vision Workshops*, 1509–1515.
- Zhu, X.; Su, W.; Lu, L.; Li, B.; Wang, X.; and Dai, J. 2020. Deformable DETR: Deformable Transformers for End-to-End Object Detection. *arXiv preprint arXiv:2010.04159*.